

Query Provenance Analysis for Robust and Efficient Query-based Black-box Attack Defense

Shaofei Li*, Ziqi Zhang[†], Haomin Jia[‡], Ding Li*, Yao Guo*, Xiangqun Chen*

*Key Laboratory of High-Confidence Software Technologies (MOE), School of Computer Science, Peking University

[†]University of Illinois Urbana-Champaign

[‡]School of Electronics Engineering and Computer Science, Peking University

{lishaofei,ding_li,yaoguo,cherry}@pku.edu.cn,

ziqi24@illinois.edu, stevenjia@stu.pku.edu.cn

Abstract—Query-based black-box attacks have emerged as a significant threat to machine learning systems, where adversaries can manipulate the input queries to generate adversarial examples that can cause misclassification of the model. To counter these attacks, researchers have proposed Stateful Defense Models (SDMs) for detecting adversarial query sequences and rejecting queries that are “similar” to the history queries. Existing state-of-the-art (SOTA) SDMs (e.g., BlackLight and PIHA) have shown great effectiveness in defending against these attacks. However, recent studies have shown that they are vulnerable to Oracle-guided Adaptive Rejection Sampling (OARS) attacks, which is a stronger adaptive attack strategy. It can be easily integrated with existing attack algorithms to evade the SDMs by generating queries with fine-tuned direction and step size of perturbations utilizing the leaked decision information from the SDMs.

In this paper, we propose a novel approach, Query Provenance Analysis (QPA), for more robust and efficient SDMs. QPA encapsulates the historical relationships among queries as the sequence feature to capture the fundamental difference between benign and adversarial query sequences. To utilize the query provenance, we propose an efficient query provenance analysis algorithm with dynamic management. We evaluate QPA compared with two baselines, BlackLight and PIHA, on four widely used datasets with six query-based black-box attack algorithms. The results show that QPA outperforms the baselines in terms of defense effectiveness and efficiency on both non-adaptive and adaptive attacks. Specifically, QPA reduces the Attack Success Rate (ASR) of OARS to 4.08%, comparing to 77.63% and 87.72% for BlackLight and PIHA, respectively. Moreover, QPA also achieves 7.67x and 2.25x higher throughput than BlackLight and PIHA.

1. Introduction

Machine Learning (ML) is extensively employed in various applications, including face recognition [2], [45], autonomous driving [15], [30] and medical image annotation [19], [46]. However, recent research has revealed that Deep Neural Networks (DNNs) are vulnerable to adversarial examples [5], [18], [35], [40], which are maliciously crafted

inputs with small perturbations and can cause the DNNs to behave abnormally. Researchers have recently proposed various strategies for generating adversarial examples, categorizing them into white-box attacks [33], [41] and black-box attacks [39], [48]. White-box attacks presuppose complete knowledge of the target DNNs, including its architecture and parameters. Conversely, black-box attacks assume no knowledge of the target DNNs, with attackers only able to query the target DNNs for outputs, such as a full probability distribution across labels or merely the predicted label. While white-box attacks can more effectively compromise DNNs, black-box attacks are more practical in real-world scenarios, such as Machine Learning as a Service (MLaaS) [3], [10], [37]. In MLaaS, service providers offer DNNs models as a service to users, who can only query the DNNs models for outputs and lack knowledge of the DNNs models. Consequently, attackers can only launch black-box attacks against the DNNs models. Several query-based black-box attacks have been proposed to construct adversarial examples [4], [5], [6], [18], [27], [31], [44]. These attacks can achieve nearly a 100% success rate and serve as foundational techniques for adversarial-based attacks [9], [20], [21], [32], [42], [49] against DNNs models.

To defend against the query-based black-box attacks, researchers have proposed SDMs [7], [8], [12], [28]. Considering that these attacks require querying the DNNs with multiple similar inputs with bounded perturbations, SDMs are designed to detect adversarial examples by individually monitoring each new query instance’s similarity with the previous query history, identifying the most similar query, and comparing their similarity with a threshold. Although existing SDMs can effectively detect attacks in certain scenarios, recent research has exposed their instability in defending against query-based black-box attacks, leading to the proposal of a stronger adaptive attack, OARS [13]. Unlike previous adaptive attacks that apply simple transformations to input queries, OARS employs adaptive methods to learn the decision boundary of SDMs based on the feedback, enabling the fine-tuning of the attack algorithm during the attack process to evade them.

The main reason for the vulnerability lies in the fact that existing SDMs primarily rely on the individual

feature about ONE incoming query and the decision of SDMs leaks information about the decision boundary, allowing the adversaries to design an attack samples that lies on the decision boundary. This approach leverages the similarity of the closest history query as individual feature, which overlooks the similarity information of other historical queries and makes it easier for adaptive attacks to evade the SDMs by finding the most similar queries that will not trigger the SDMs. Moreover, lowering the threshold of existing SDMs to enhance their robustness is also impractical, as it neither prevents stronger adaptive attacks nor reduces the false positive rate. Consequently, a more robust defense method is required to counteract stronger adaptive attacks.

Our key insight is that *detection on sequence feature, joint analysis of historical queries, is more robust than that on the individual features*. Attack sequences can form certain unique patterns due to the consecutive construction of anomalous query sequences with small perturbations, while normal query sequences lack such patterns. Although adaptive attacks, such as OARS, can evade single-point detection, they cannot conceal the anomaly of the entire query sequence. OARS can evade existing SDMs by finding the most similar queries that will not trigger the SDMs, but the similarity among instances in the query sequence remains. Therefore, we can detect query-based black-box attacks based on sequence features.

Intuitively, one might employ clustering algorithms and sequence models to leverage sequence features. Clustering algorithms could use similarity as distance, categorizing queries to identify anomalous clusters. However, these algorithms face scalability issues with chaotic and noisy data [17], leading to misclassifications and compromised detection accuracy in MLaaS scenario. While sequence models, such as Recurrent Neural Network (RNN) and Long Short-Term Memory (LSTM), can capture sequence features, they are susceptible to long-running attacks [22], [34], rendering them unsuitable for detecting query-based black-box attacks. Hence, these methods are not applicable for detecting query-based black-box attacks.

This paper introduces Query Provenance Analysis (QPA), a novel defense method against query-based black-box attacks. QPA aims to robustly detect anomalous queries in real-time with fewer false positives. It leverages the sequence feature of query instances, termed as query provenance, to detect these attacks. Unlike clustering algorithms, QPA integrates both similarity and structural features to form the basis of query provenance, enhancing attack detection accuracy even for noisy data. For attack-related queries, the query provenance is the preceding query sequence involved in constructing the query instance. Normal queries, lacking a relationship with other queries, do not possess the provenance feature. To better characterize query relationships, we represent the provenance of queries as a graph structure. When a new query arrives, we select the most similar query as its ancestor and link them with a weight representing their similarity. QPA can then detect query-based black-box attacks based on the provenance graph of each new query instance. If a query instance's provenance is

abnormal, it is detected as an anomalous query. Compared to existing SDMs, QPA can more robustly detect query-based black-box attacks, as it utilizes the fundamental anomaly of query-based black-box attack query sequences.

However, the design of QPA is a non-trivial design problem. The key challenge of QPA is how to recognize attack query sequences effectively in massive noisy queries in real time. On the one hand, compared with previous methods, QPA introduces graph structure for robust anomaly detection to achieve better effectiveness, which will bring additional overhead for graph computation. Therefore, how to efficiently determine whether the provenance of a query is anomalous is quite challenging. To achieve this goal, we design an anomaly detection algorithm based on a combination of statistics analysis and Graph Neural Networks (GNNs) classifier. The statistics analysis can exclude most of the normal queries by similarity aggregation. Then the GNNs classifier can filter out the false positives based on the provenance graph structure features. On the other hand, the attacks can be intermittent, which means that the attack procedure can last for a long time and be mixed with normal queries. QPA requires the provenance of each query instance to detect the attack. However, as the query stream arrives, the size of the provenance graphs increases and it is impossible to keep all the query provenance information in the memory. To address this problem, we deploy a graph eviction strategy to hold the suspicious provenance graphs and evict the normal graphs into the disks.

In summary, our main contribution is the proposal of QPA, a novel and effective defense method against query-based black-box attacks on DNNs. Unlike existing SDMs that rely on individual query similarities, QPA leverages the provenance of query sequences to identify anomalous behavior. This approach is grounded in the insight that the sequence feature of attacks provides a more robust anomaly detection mechanism compared to single instance analysis. We summarize our major contributions as follows:

- We propose QPA, a novel defense method against query-based black-box attacks that leverages the provenance of query sequences to identify anomalous query sequences.
- We evaluate QPA on non-adaptive and adaptive attacks on four widely-used image datasets and demonstrate that QPA outperforms existing SDMs in terms of detection accuracy, robustness and efficiency.
- We release the source code of QPA at <https://anonymous.4open.science/r/QPA-6063/> to facilitate further research on adaptive attacks and SDMs in this area.

2. Background and Motivating Example

In this section, we will introduce the background of our work, including query-based black-box attacks, existing SDMs defenses, and adaptive attacks. We will then present a motivating example to illustrate the insight of QPA and its challenges.

2.1. Query-based Black-Box Attack

Query-based black-box attacks are a class of adversarial attacks that only require query access to the target model. The attackers can repeatedly query the target model with crafted inputs and get the corresponding outputs. Considering the types of output information, the query-based black-box attack algorithms can be divided into two types: score-based attacks and decision-based attacks. Score-based attack [4], [18] requires the attacker to know all the probabilities over the whole label space. Decision-based attack [5], [6], [27], [31] only needs the predicted label. Both of the two types of attacks start from an original input and iteratively perturb the input to generate adversarial examples so that they can be falsely classified as a targeted or untargeted label. The average number of queries to a successful attack is used to measure the efficiency of query-based black-box attack algorithms. A successful attack usually requires hundreds to thousands of queries. The general pipeline of query-based black-box attack algorithms consists of three elements: Gradient Estimation, Step Execution, and Boundary Identification.

① Gradient Estimation. Given an attack point x_t , each step starts from a gaussian noise vector δ_t that has the same size of x_t . The attacker then queries the target model f with $x_t + \delta_t$ to get the corresponding output. For each iteration of estimation, the attacker generates n noise vector and the gradient can be estimated by

$$\nabla_x f(x_t + \delta_t) \approx \frac{1}{n} \sum_{i=1}^n L(f(x_t + \delta_{t_i}), f(x_t)), \quad (1)$$

where L is the loss function and different algorithms have different strategies.

② Step Execution: Once the gradient has been estimated, the attack algorithms perturb the start point x_t to x'_t by taking a step in the gradient's direction. The step size is typically initialized based on the current iteration round number and attack algorithms often employ the binary search algorithm to find an appropriate step size to improve convergence.

③ Boundary Identification: Some attack algorithms update the x'_t by linearly interpolating between the itself and the original victim sample x_{vic} . This interpolation shifts x'_t closer to the decision boundary, thereby selecting a more favorable starting point for the subsequent iteration. The interpolation procedure is conventionally guided by the binary search algorithm, which navigates the parameter space between x'_t and x_{vic} to get more close to the decision boundary of target model.

2.2. Stateful Defense Models

To defend against query-based black-box attacks, researchers have proposed various defense SDMs based models [7], [8], [12], [28]. The key insight behind SDMs is that query-based black-box attacks need to generate many very similar queries in the stages of gradient estimation

and boundary identification. Thus, we can detect query-based black-box attacks by detecting queries that show high similarities.

The existing approaches are *individual similarity-based SDMs* approaches [7], [8], [12], [13], [28]. These approaches compare ONE incoming query to EACH INDIVIDUAL query in the history and mark the incoming query skeptical if the is very similar (e.g., the similarity is higher than a predefined threshold) to another query in the history. However, the detection relying solely on individual similarity comparison has two significant limitations. First of all, it lacks stability, as it can introduce false positives because normal queries may still show high similarity. Second, it is less robust, as the individual similarity-based method is vulnerable to more advanced adaptive attacks. Recent research has shown that advanced adaptive attacks can fine-tune the direction and step size of perturbations to ensure that the similarity between queries does not collide with the threshold-based decision boundary [13], which we will introduce in detail in the following subsection.

2.3. Adaptive Attacks

Current individual similarity-based SDMs have been demonstrated susceptibility to adaptive attacks. These attacks strategically manipulate the similarity between queries to avoid intersecting with the threshold-based decision boundary. Generally, existing adaptive attacks can be divided into two categories: query-blinding strategy [7] and adapt-and-resample strategy [13].

The query blinding strategy aims to ascertain the output of the target model while concealing the initial query from the defense model. This strategy employs common image transformation techniques such as rotation, translation and brightness adjustment so it can be easily applied without modifying the attack algorithm itself. However, this strategy often influences the attack's efficacy, potentially resulting in a successful evasion at the expense of the attack's failure [13]. The adapt-and-resample strategy called OARS, is more sophisticated and does not just transform images. It utilizes the leaked information of the defense model to perform rejection sampling that can perceive the discriminant boundary and adaptively adjust the attack parameters to escape detection. It utilizes binary search to find the optimal step size and noise distribution to generate queries that are most similar to the previous queries but will not cause collision. It is a general approach that can be applied to any attack consisting of the above three attack elements. The OARS is an advanced adaptive attack compared with the query blinding because it leverages the leaked information of the defense model to adjust the attack direction adaptively but the query blinding strategy is aimless.

Although different adaptive strategy has different attack performances, they all bypass the detection of existing SDMs by circumventing the threshold-based decision boundary. Therefore, the individual feature-based SDMs is not robust enough to detect adaptive attacks. To address this challenge, we propose to utilize sequence features instead

of individual features to enhance the detection capability of SDMs. We will demonstrate why sequence features are more robust using an example in the following subsection.

2.4. Key Insight

In light of the limitations of current SDMs, we propose a novel approach that leverages sequence features, rather than individual features, to bolster the robustness of SDMs. This approach is based on our observation that the attack query sequences are aggregated in a highly structured pattern, a characteristic absent in benign query sequences.

As detailed in Section 2.1, typical query-based black-box attack algorithms create adversarial examples by iteratively modifying inputs through three key elements: Gradient Estimation, Step Execution, and Boundary Identification. In the Gradient Estimation phase, the attacker crafts multiple queries from a current attack point to estimate the gradient. The attacker then updates the attack point in the Step Execution and Boundary Identification phase, taking a step in the direction indicated by the gradient with interpolation to approach the boundary. The attack sequence, therefore, shows a spread (broad sampling of queries) and advance (progressive movement towards the boundary) pattern in each iteration. As the attack proceeds, the query sequence forms a highly organized tree structure with the spread-and-advance pattern. This pattern is based on the similarity-based historical relationships among queries and is consistent across different attacks. Even though not all attack algorithms incorporate all three elements, the attack sequence still manifests its unique pattern. Such sequence features are robust against adaptive attacks like OARS. This is because OARS follows the three-element methodology, generating queries that exhibit higher similarity compared to normal queries. As a result, these sequence features maintain the ability to distinguish attack patterns, thereby providing enhanced robustness against sophisticated adaptive strategies.

However, it is challenging to design a SDMs that can effectively capture the sequence features of queries. The primary difficulty lies in detecting attack query sequences effectively in massive noisy queries in real time. Existing research aimed at capturing sequence features for anomaly detection primarily focuses on clustering-based methods [14], [24] and sequence model [16], [29]. However, clustering-based methods are not suitable for chaotic and noisy query sequences, and sequence models are vulnerable to long-running attacks. To this end, we propose a query provenance graph to capture the sequence features of queries, which will be introduced in the following section.

3. Query Provenance Graph

Recognizing that sequence features encapsulate the historical relationships among queries, we refer to this type of feature as *query provenance* and organize the history queries as *query provenance graph*. The query provenance graph is an undirected graph $G = (V, E)$ where V is the set of nodes representing the queries and E is the set of

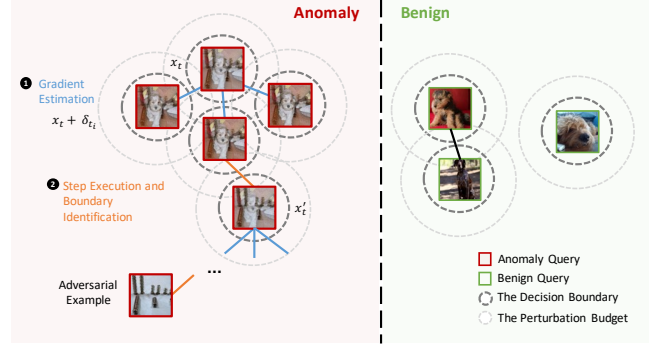


Figure 1: A motivating example of query provenance graph. x_t indicates the start point, $x_t + \delta_t$ indicates the perturbed queries and x'_t indicates the start point of the next iteration. The attack query sequence forms a highly organized graph structure while the benign query sequence shows random aggregation. Existing SDMs employ a threshold-based decision boundary to detect the attack queries, which is vulnerable to OARS that can generate queries outside the decision boundary while inside the perturbation budget.

edges with weights $\text{sim}(F(x_i), F(x_j))$ that measures the similarity between two queries x_i and x_j , where $F(x)$ is the feature extraction function. The graph is incrementally constructed as new query arrives, by adding the new query as a node and linking it to the most similar query. This concept is illustrated through an example depicted in Figure 1.

This example illustrates the generation of an adversarial example using HSJA attack [6] with OARS strategy in chaotic data. Each node represents a query and we organize the history queries as query provenance graphs by connecting the newly arrived query to the most similar previous queries. On the left side of this example, it is a consecutive process to generate an adversarial example, leading to the misclassification of a screw as a dog. On the right, benign queries are randomly aggregated. For the attack query sequence, the graph progressively expands as the attack unfolds, culminating in the successful generation of an adversarial example. Initially, the attacker crafts multiple queries $x_t + \delta_t$ from a current attack point x_t to estimate the gradient. Therefore, the query sequence forms a subgraph with a divergent structure radiating from the origin point. After estimating the gradient, the attacker updates the attack point by taking a step in the direction indicated by the gradient. Then the algorithm modifies the newly generated point by interpolating a line between it and the original victim sample to approach the boundary and establish the starting point x'_t of the next iteration. This step represents a forward move on the graph. These three steps are then repeated until the adversarial example is successfully generated.

Note that the OARS strategy can adjust the direction and step size of perturbations to generate queries outside the threshold-based decision boundary of existing SDMs, thereby evading detection. Taking advantage of the query provenance graph, the attack query sequence delineates a highly organized tree structure, a feature that OARS strat-

egy can hardly circumvent. Conversely, the benign query sequence forms a random aggregation, as shown on the right side of the example. Thus, the query provenance graph can capture the sequence features of anomalous queries and distinguish them from benign queries, which is effective for chaotic data. We can then utilize the query provenance graph to design a more robust SDMs to defend against adaptive query-based black-box attacks. The details of query provenance graph construction will be discussed in Section 5.1.

4. Threat model and Design Goal

Our threat model follows prior defense against query-based black-box attacks [28]. We consider the following assumptions in our threat model:

Attackers’ Ability. The target DNNs models are deployed as a service. The attacker has no access to the training data and the target model’s architecture and parameters. The attacker can only query the target model with valid inputs and get the corresponding outputs, a full probability distribution across labels or only the predicted label. The attacker can only generate adversarial examples by querying the target model and cannot utilize other information. The attacker can switch the attack between multiple user accounts and the cost is negligible.

Attacker’s Goal. The attacker aims to generate adversarial examples that can cause the target model to misclassify the original inputs. The attacker can use any query-based black-box attack algorithm to generate adversarial examples to achieve high success rate and low query cost.

Defenders’ Ability. The defender has access to the target model’s inputs and outputs. The defender does not need to know model architecture or internal state. The defender has limited resources for defense, such as computation and storage, which means that the continually increasing resource consumption is not acceptable.

Defenders’ Goal. Our goal to defense against query-based black-box attacks is three-fold:

- **Robustness.** The defense model should be robust against both non-adaptive and adaptive attacks, especially for stronger adaptive attack, e.g., OARS.
- **Accuracy.** The defense model is designed to accurately detect and defend against the generation of adversarial examples, ensuring high coverage and a low false positive rate. It should be capable of identifying adversarial examples generated by various query-based black-box attacks. Furthermore, the model is designed to adapt to real-world scenarios, where normal queries significantly outnumber attack-related queries.
- **Efficiency.** The defense model should be efficient and introduce little latency in the responding period. The defense solution should be scalable to large-scale systems. The defense model should be able to handle a large number of queries in real-time and introduce little latency to the response of queries.

5. Design

We propose to leverage query provenance for online query-based black-box attack detection, as depicted in Figure 2. Our system comprises two main components: graph construction and query provenance analysis. The former constructs the query provenance graph based on the similarity between queries, while the latter analyzes these query provenance graphs to detect anomalous sequences. To detect long-running attacks in chaotic environments, we implement a two-phase detection mechanism: statistics analysis and graph classifier. The statistics analysis is lightweight and efficient and filters out suspicious query provenance graphs. The graph classifier improves detection accuracy by classifying the outputs of the statistics analysis. We also incorporate a dynamic management strategy of query provenance graphs, including graph eviction and reset. Graph eviction maintains a suspicious query history in memory and evicts normal queries to the disk database. Graph reset periodically resets graph storage to maintain system efficiency. The design of each component is detailed in the following subsections.

5.1. Graph Construction

The graph construction component takes a query stream as input and arranges the query history in a graph structure. It builds the query provenance graph incrementally, utilizing the similarity between queries calculated from query features extracted by the feature extractor.

Similarity Calculation. In our system, we utilize the feature extractor $F(x)$ from PIHA [8] as the default method to extract features from the query x and compute the similarity between queries based on these features. PIHA employs the Locality Sensitive Hashing (LSH) for feature extraction and preserves a fixed number of hash values as the query features. It uses the Gaussian filter and LBP algorithm as the feature extractor $F(x)$, as they are more resilient and efficient against adversarial perturbations compared to BlackLight’s extractor. The similarity function is defined as

$$\text{sim}(F(x_i), F(x_j)) = \frac{F(x_i) \cap F(x_j)}{|F(x)|},$$

where $F(x_i) \cap F(x_j)$ denotes the common hash values between the features of x_i and x_j and $|F(x)|$ denotes the size of the features.

Graph Initialization. Attack queries tend to form highly structured query provenance graphs, a trait not common to normal queries. This difference is crucial, allowing for effective classification of suspicious query provenance during the QPA phase. However, normal queries can introduce random aggregation into the query provenance graph, which may result in false positives. To mitigate this, we pre-initialize the graph with a small set of normal queries, typically 1,000, as distinct nodes. This approach decreases the chances of normal queries linking within the same graph. These normal queries are chosen either from the normal set or from those already processed by the target model. To maintain diversity

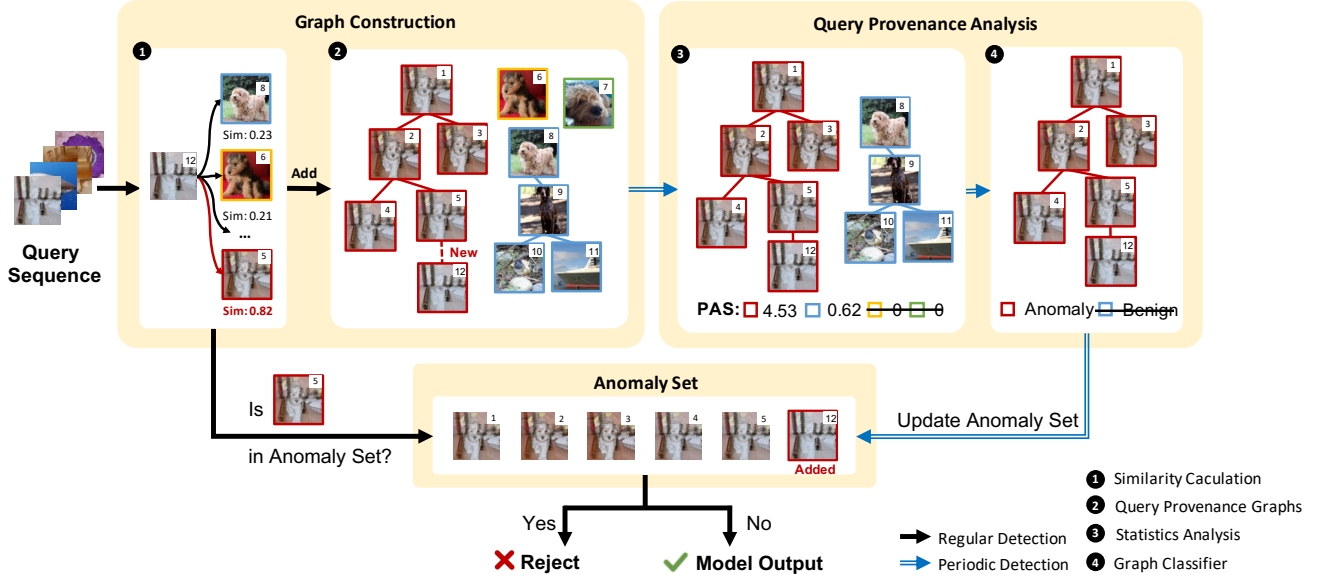


Figure 2: Workflow of the our system with QPA. The system receives the query stream as input and constructs the query provenance graph based on the similarity between queries. It analyzes the query provenance graph to update the anomaly set periodically. As a result, it rejects the anomalous queries and returns model outputs for benign ones.

among normal queries, we select from different classes for certain datasets.

Incremental Construction. The query provenance graph is constructed incrementally as the new query arrives. A straightforward approach would be to add the incoming query as a node in the graph and connect it to the most similar queries. However, this method may introduce false positives because the normal queries may have the highest similarity to attack queries with extremely small similarity, complicating subsequent detection. To mitigate this issue, we set a threshold T for the similarity based on the observation that the similarity between attack queries significantly exceeds that between entirely unrelated images. If the similarity between the incoming query and the most similar query falls below this threshold, we only add the incoming query as a node without connecting them with an edge. We set the threshold T to the *90th percentile* similarity between the normal queries used in the initialization. We compare the detection performance with and without T in Section 6.5.

5.2. Query Provenance Analysis (QPA)

The QPA is used to analyze the query provenance graphs and detect the anomaly sequences. It receives the query provenance graphs as input and detects the anomaly graph as anomaly set. QPA detects anomalies based on the Provenance Anomaly Score (PAS) and the structure of the query provenance graph. To guarantee the detection accuracy and efficiency, we adopt a two-phase detection mechanism: 1) Statistics Analysis and 2) Graph Classifier. Statistics analysis calculates the PAS for each query provenance graph to filter out the suspicious graphs. Then the graph classifier utilizes GNNs to classify the outputs of the statistics analysis based on their PAS and graph structure. Instead of directly

using the graph classifier, we use the statistics analysis to filter out the suspicious graphs to reduce the computation overhead of the graph classifier.

Statistics Analysis. In the statistics analysis, we calculate the PAS for each connected query provenance graph. The PAS is used to represent the sequence similarity of the query provenance graph. Considering the attack query sequence is generated by continuously perturbing the input, the sequence similarity of attack sequence is higher than the normal ones. Thus we can utilize the PAS to detect the anomaly.

We calculate the PAS based on the similarity weight assigned to the edges between queries in the graph. This weight corresponds to the similarity between queries and their closest neighbors, established during the construction of the query provenance graph. One might initially consider defining PAS as the average of all the edges in the graph. However, this approach fails to robustly differentiate anomalous from normal query sequences, especially for adapt-and-resample adaptive attacks. These attacks can identify directions and step sizes that minimize similarity, thereby reducing the distinctiveness of the similarity between queries. Thus the average similarity overlooks the query provenance graphs' scale feature, which means that the nodes of the attack query provenance graph significantly outnumber those of normal ones. To distinguish between attack and normal queries more effectively, we define PAS as the sum of all edge weights in a connected graph, formally expressed as $PAS(G) = \sum_{e \in G} e_{weight}$. Even for adaptive attacks, the attack sequence will exhibit an extremely higher PAS compared to normal ones due to the high degree of aggregation.

To identify anomalies based on the PAS, we employ the Grubbs's test [1], a statistical algorithm designed to detect outliers within a sample set. Specifically, the Grubbs's test

can determine whether the largest value in a set of samples is an outlier. Grubbs’s test is defined for the following hypotheses:

$$G_{test} = \frac{Y_{max} - \bar{Y}}{s}$$

$$G_{critical} = \frac{N - 1}{\sqrt{N}} \sqrt{\frac{t_{\alpha/N, N-2}^2}{N - 2 + t_{\alpha/N, N-2}^2}}$$

with \bar{Y} and s denoting the mean and standard deviation of the samples, $t_{\alpha/N, N-2}$ denoting the upper critical value of the t-distribution with $N - 2$ degrees of freedom and a significance level of α/N . The null hypothesis, which posits the absence of outliers, is rejected at the significance level α if $G_{test} < G_{critical}$. In our system, we set the significance level $\alpha = 0.01$ for fewer false positives.

We selected Grubbs’s test due to its lightweight nature and robustness in this scenario. We apply Grubbs’s test to the query history iteratively until no outliers are identified. However, the detected outliers may contain false positives, which reduces detection accuracy. To address this, we incorporate a graph classifier to further categorize the outputs of the statistical analysis based on their PAS and graph structure.

Graph Classifier. The graph classifier is designed to reduce the false positives of the statistics analysis, leveraging both PAS and graph structure. In real-world scenarios, normal queries significantly outnumber attack queries, potentially leading to random aggregation in the query provenance graph. However, these aggregations do not form a highly structured graph as the attack sequence. Based on this observation, we can combine PAS and graph structure to improve detection accuracy.

We employ GNNs to learn graph embeddings and train a binary classifier for classification. GNNs are powerful tools for capturing graph structure and node features. A straightforward approach is to use the original query provenance graph as the GNNs input. However, this graph only contains edge features, and traditional GNNs such as Graph Convolutional Networks (GCN) [50] and Graph Attention Networks (GAT) [43] are based on node features, leading to suboptimal learning performance for embeddings. To overcome this issue, we transform the original graph into its line graph [47]. A line graph represents the edges of the original graph as nodes, and the edges between these nodes represent the adjacency of the original graph. This transformation allows the line graph to capture both the graph structure and edge features simultaneously. We then feed the line graph into the classic GCN model to learn the graph embedding and perform classification. The loss function is defined as the cross-entropy loss between the predicted label and the ground truth. The graph classifier model comprises three convolutional layers and one linear layer, offering a lightweight structure that introduces minimal latency for online detection.

The graph classifier is pretrained offline and deployed for online detection. We impose a limit, denoted as s , on

the node count of the input graph. This constraint ensures that the graph’s structural characteristics are adequately represented, as these characteristics only become apparent when the graph reaches a certain scale. The parameter s influences both the Time-To-Detect (TTD), which is defined as the number of queries to detection, and detection accuracy, which we will discuss in Section 6. The graph classifier is trained on randomly selected attack sequences and normal queries, with each dataset trained independently. For anomaly samples, we randomly select five attack sequences for each attack algorithm and construct the query provenance graphs. We then save the graph as a sample for every s queries. For normal samples, we randomly select the normal queries from the normal set. Given that normal queries exhibit less aggregation than attack queries, we save a graph sample for every 500 queries. Subsequently, we partition the dataset into training and testing sets at a ratio of 7:3. The graph classifier is trained using the training set, and the best-performing model on the testing set is saved for online deployment.

5.3. Dynamic Management

System efficiency is crucial for ML services. The query provenance graph, which may expand indefinitely with incoming queries, can introduce significant computational overhead for detection. To counteract long-running adversarial attacks while ensuring the efficiency of ML service, we design an eviction strategy to maintain the suspicious query history in memory while evicting the normal queries to a database on disk. This approach differs from previous SDMs, which retain all query features in memory. Instead, our strategy selectively retains only the more suspicious query provenance graphs, while efficiently offloading the normal ones to the database. We also design a graph reset strategy to periodically reset the query provenance graph storage. We integrate these dynamic management strategies in the periodic detection to maintain the integrity and performance of the system.

Graph Eviction. In our design of QPA, the query provenance is organized as an undirected graph, with each connected query provenance graph assigned a PAS to represent the sequence similarity. A higher PAS indicates greater sequence similarity of the query provenance graph and the attack sequences will have extremely higher PAS compared to the normal ones. Intuitively, we can preserve the graphs with the top K highest PAS in the memory and evict the others to the database. This approach would reduce computational overhead for detection, as we would only need to calculate the similarity with the suspicious query history. In real scenarios, attack queries are far fewer than normal queries and exhibit aggregation in the query provenance graph, suggesting that the number of attack-related graphs is limited. Therefore, we can preserve only the top K highest PAS graphs in the memory after the QPA phase to facilitate subsequent detection. To ensure the detection capability, we preserve the graph structure in the database for integrated analysis between time windows by connecting the evicted

TABLE 1: The configurations and performance of six SOTA non-adaptive attacks without any defense. “ASR” indicates the attack success rate and “Avg # of queries” indicates the average number of queries to generate an adversarial example.

Attack	Targeted	Distance	ASR				Avg # of queries			
			MNIST	CIFAR10	ImageNet	CelebaHQ	MNIST	CIFAR10	ImageNet	CelebaHQ
NES	Targeted	L_∞	40%	100%	99%	100%	49570	707	14324	6737
Boundary	Untargeted	L_2	73%	100%	100%	100%	15190	605	6468	730
Square	Untargeted	L_2	98%	100%	100%	100%	5731	390	346	632
HSJA	Targeted	L_2	82%	100%	100%	100%	1890	1246	13237	7956
QEBA	Targeted	L_2	98%	99%	53%	100%	2194	2620	15425	3948
SurFree	Untargeted	L_2	74%	100%	100%	100%	10344	167	645	191

nodes to the closest nodes in the database. The eviction procedure is asynchronous with online detection, ensuring it does not impact detection efficiency. We will discuss the impact of K in Section 6.5.

Graph Reset. Limited by the resources for defense, the query provenance graph cannot grow infinitely. Therefore we reset the storage of graphs per 24 hours to maintain the efficiency of the system. We reset the query provenance graphs by purging the memory and database, then reinitialize the query provenance graph with the normal queries. However, it may provide an opportunity for long-running attacks to escape detection. We will discuss the evasion of attacks in Section 7.

6. Evaluation

We evaluate our system with six non-adaptive attacks and their OARS versions [13] on four widely used datasets: MNIST [11], CIFAR10 [25], ImageNet [38] and CelebaHQ [23]. We compare our QPA-based SDMs with two state-of-the-art SDMs: BlackLight [28] and PIHA [8]. Our QPA-based system is designed to achieve robustness and efficiency at the same time. Therefore, we proposed the following research questions to evaluate QPA-based SDMs:

- **RQ1:** Can QPA detect and defend against query-based black-box attacks more effectively than existing SDMs?
- **RQ2:** Can QPA detects query-based black-box attacks efficiently?
- **RQ3:** Does QPA utilize query provenance to detect query-based black-box attacks?
- **RQ4:** How do the hyperparameters and each technique affect the detection performance of QPA?

In this section, we will first introduce the experimental setup in Section 6.1. Then, we will display the effectiveness of QPA in front of both adaptive and non-adaptive attacks in Section 6.2. In Section 6.3 and Section 6.4, we will display the efficiency of QPA and verify our insight. At last, in Section 6.5, we will study the influence of hyperparameters and each component.

6.1. Experimental Setup

Our experiments focus on the image classification tasks, which are the most widely used tasks in previous work.

TABLE 2: Overview of image classification task configurations.

Dataset	Model Architecture	Model Accuracy
MNIST	6 Conv + 3 Dense	99.36%
CIFAR-10	ResNet20	91.73%
ImageNet	ResNet152	78.31%
CelebaHQ	ResNet152	89.55%

To ensure evaluation fairness, we choose the datasets and targeted models that previous work has used [13], [28].

Image Classification Tasks. We evaluate the defense performance of BlackLight and PIHA on the four most common datasets: MNIST, CIFAR10, ImageNet and CelebaHQ. For MNIST, we trained a LeNet-5 [26] convolutional network for digital number classification. For CIFAR10, ImageNet and CelebaHQ, we selected the targeted models that previous work has used [13]. Table 2 lists the details of the datasets and targeted models.

Baseline Configurations. As discussed in Section 2.2, we choose two global query store design SDMs as our baselines: BlackLight [28] and PIHA [8]. We use the open-source implementation and most of the default configurations of BlackLight and PIHA as described in their papers. For BlackLight, we configured its hyperparameters for different datasets as listed in the paper and set the same hyperparameters for CelebaHQ as ImageNet. We set the similarity threshold $q = 0.5$ for BlackLight. For PIHA, we adjust the similarity threshold q , which is the proportion of identical hash values in a hash sequence, from 0.95 to 0.8 to achieve the best performance.

Attack Configurations. We evaluate QPA-based SDMs with six non-adaptive query-based black-box attacks and deploy query-blinding and OARS strategies for these non-adaptive attacks to evaluate the robustness of our system against adaptive attacks.

We selected six SOTA non-adaptive attacks: NES [18], Boundary [5], Square [4], HSJA [6], QEBA [27] and Surfree [31]. NES and Square are score-based attacks that need to get a full probability distribution across labels and the others are decision-based that only require the output label. We use the open-source implementation of the attacks and the default configurations. We set the normalized perturbation budgets $\sigma = 0.05$ as prior work used. The only exception is we set $\sigma = 0.1$ for the attacks on MNIST since it is necessary for them to succeed within a limited time.

TABLE 3: Our detection system with QPA outperforms existing SDMs on non-adaptive attacks. BL and PIHA indicate our two baseline BlackLight and PIHA. We can find that our system has the best detection performance on average. The best results are in bold.

Dataset	Attack	Detection Coverage			Detection Precision			FPR			TTD		
		BL	PIHA	QPA	BL	PIHA	QPA	BL	PIHA	QPA	BL	PIHA	QPA
MNIST	NES	0.98	-	0.95	1.00	-	1.00	0.00%	-	0.00%	2.1	-	20.3
	Boundary	0.60	-	0.99	0.04	-	1.00	13.00%	-	0.00%	2.4	-	20.3
	Square	0.99	-	1.00	1.00	-	1.00	0.00%	-	0.00%	2.0	-	18.5
	HSJA	0.94	-	0.97	1.00	-	1.00	0.00%	-	0.00%	5.0	-	21.2
	QEBA	0.83	-	0.88	1.00	-	1.00	0.00%	-	0.00%	8.1	-	23.4
	SurFree	0.03	-	1.00	0.52	-	1.00	0.08%	-	0.00%	6.0	-	20.1
CIFAR10	NES	0.97	0.98	0.99	0.97	0.74	0.90	0.04%	0.36%	0.16%	2.0	2.5	18.9
	Boundary	0.21	0.75	0.94	0.86	0.61	0.96	0.05%	0.47%	0.03%	2.5	2.5	20.5
	Square	0.99	0.96	1.00	0.97	0.85	0.93	0.03%	0.19%	0.10%	2.0	2.0	18.0
	HSJA	0.95	0.97	0.89	0.96	0.69	0.91	0.04%	0.44%	0.18%	4.9	2.3	19.3
	QEBA	0.95	0.97	0.76	0.96	0.68	0.89	0.04%	0.46%	0.13%	5.1	2.5	19.3
	SurFree	0.07	0.53	0.81	0.59	0.69	0.91	0.09%	0.22%	0.03%	10.3	7.1	45.2
ImageNet	NES	0.98	0.90	0.99	0.88	0.89	1.00	0.14%	0.10%	0.00%	2.1	9.3	17.7
	Boundary	0.03	0.35	0.99	0.18	0.78	0.98	0.14%	0.10%	0.03%	9.4	2.0	18.6
	Square	0.98	0.98	0.99	0.92	0.97	1.00	0.09%	0.04%	0.00%	2.0	2.0	17.8
	HSJA	0.95	0.95	0.98	0.87	0.91	0.98	0.14%	0.10%	0.00%	6.2	5.7	17.7
	QEBA	0.94	0.95	0.97	0.88	0.91	0.96	0.13%	0.09%	0.06%	7.5	5.9	18.8
	SurFree	0.05	0.06	0.99	0.30	0.50	1.00	0.11%	0.05%	0.00%	7.7	6.1	18.4
CelebaHQ	NES	0.97	0.92	1.00	0.92	0.92	1.00	0.08%	0.08%	0.00%	2.1	9.9	18.9
	Boundary	0.01	0.69	0.99	0.09	0.90	1.00	0.09%	0.08%	0.00%	11.4	2.0	19.2
	Square	0.99	0.99	1.00	0.95	0.95	1.00	0.06%	0.05%	0.00%	2.0	2.2	18.7
	HSJA	0.92	0.92	0.99	0.92	0.92	1.00	0.08%	0.07%	0.00%	6.2	5.6	17.9
	QEBA	0.92	0.85	1.00	0.92	0.91	1.00	0.08%	0.07%	0.00%	6.1	11.8	18.0
	SurFree	0.16	0.14	0.99	0.77	0.72	1.00	0.03%	0.03%	0.00%	8.2	8.4	18.2
	Avg	0.71	0.77	0.96	0.77	0.81	0.98	0.77%	0.17%	0.04%	5.14	4.99	20.20

Table 1 lists the configurations of the non-adaptive attacks and the attack performance of them. For each configuration, we randomly select 100 images from the corresponding dataset. We run an attack on each instance until it terminates within 100K queries. As shown in Table 1, these attacks can achieve success within 50K queries for each instance. However, some instances still failed to generate adversarial examples even after 100K queries and we regard them as failed attacks.

For the adaptive attacks, we deploy two strategies on the above six non-adaptive attacks: query-blinding and OARS. For query-blinding, we use standard attack configurations and deploy the standard random affine transformation to blind the queries by rotation, shifting and scaling. We set the rotation angle up to 10 degrees, shifting up to 10% horizontally/vertically, and zooming up to 10%. For OARS, it modifies the standard attack algorithms with an adapt-and-resample strategy. We use the open-source implementation and the default configurations of OARS. Due to

OARS utilizing the leaked information of the decision of the defense model to adjust the attack direction and step size, we integrate our QPA-based SDMs behind it. This integration allows us to return the decision for each input query throughout the entire attack procedure.

QPA Configurations. By default, we employ the feature extraction algorithm of PIHA due to its effectiveness and efficiency. However, the feature extraction algorithm of PIHA is specifically designed for the three-channel images. When applied to the single-channel images of the MNIST dataset, we attempted to superimpose single-channel images into three-channel images but the results were suboptimal. Therefore, we use the feature extraction algorithm of BlackLight for the MNIST dataset. We preserve top $K = 20$ query provenance graphs in the memory and conduct detection on the graphs with more than $s = 15$ nodes. We will discuss the setting of our hyperparameters in Section 6.5.

6.2. Effectiveness

Non-adaptive Attacks. We evaluate the detection performance of QPA on the non-adaptive attacks in the simulated real-world environment, where the normal queries are much more than attack queries. We set the anomaly rate of the input sequence as 1% to simulate the less adversarial environment [36] and we limited the maximum number of queries to 50K. Our two baselines have shown that they have promising performance on the non-adaptive attacks in their papers and they can make these non-adaptive attack algorithms achieve a 0% attack success rate. We compare the detection coverage, detection precision, False Positive Rate (FPR), and the TTD of QPA with BlackLight and PIHA. Table 3 shows the detection performance of QPA on the non-adaptive attacks. For each row in the table, we randomly sample 100 instances from the dataset and calculate the average number.

Overall, QPA achieves the best performance on detection coverage, detection precision and FPR on average. Our system achieves an average of 96% detection coverage, 97% detection precision and 0.04% FPR, maintaining similar results across various datasets and attack algorithms. Conversely, BlackLight and PIHA exhibit significant performance fluctuations, particularly in detecting Boundary and SurFree attacks. This is attributed to their excessively high thresholds for Boundary and SurFree, highlighting the unstable performance of individual similarity-based SDMs. While the average number of queries to detection for QPA is 20.20, slightly higher than BlackLight and PIHA, it’s important to note that existing attacks necessitate hundreds to thousands of queries for a successful attack, as outlined in Table 1. Therefore, the results demonstrate that QPA can effectively detect non-adaptive attacks with high efficiency and robustness.

Adaptive Attacks. We evaluate the detection performance of QPA on the adaptive attacks with two strategies: query-blinding and OARS. Because OARS leverages the leaked information of the decision of the defense model to adjust the attack direction and step size, we integrate QPA and our two baselines for the defense to return the decision for each input query while attacking. We record the ASR to show their defense performance. Table 4 shows the detection performance of QPA and our two baselines on the adaptive attacks. We randomly sample 100 instances from the corresponding dataset for each attack configuration.

For query-blinding strategy, our two baselines demonstrate substantial defense performance against adaptive attacks. However, QPA outperforms them, achieving an average ASR of 0.29%. BlackLight and PIHA exhibit poor defense performance against the Boundary attack, aligning with the results of non-adaptive attacks. For OARS strategy, QPA can reduce the ASR of the adaptive attacks to 4.08% on average, which is much lower than the defense of the two baselines. QPA achieves the best defense performance across all the attack algorithms and datasets. The attacks always terminate within 100K queries because they cannot find any available direction and step size to take the next

TABLE 4: Our system with QPA outperforms existing SDMs on adaptive attacks. We can find that our system has the best defense performance. The best results are in bold.

Dataset	Attack	Query Blinding			OARS		
		BL	PIHA	QPA	BL	PIHA	QPA
MNIST	NES	0%	-	0%	2%	-	0%
	Boundary	0%	-	0%	69%	-	8%
	Square	0%	-	0%	55%	-	7%
	HSJA	0%	-	0%	76%	-	10%
	QEBA	0%	-	0%	87%	-	6%
	SurFree	7%	-	0%	71%	-	0%
CIFAR10	NES	0%	0%	0%	99%	83%	0%
	Boundary	0%	0%	0%	98%	90%	0%
	Square	0%	0%	0%	93%	99%	20%
	HSJA	0%	0%	0%	82%	76%	5%
	QEBA	0%	0%	0%	98%	95%	18%
	SurFree	5%	4%	2%	81%	67%	6%
ImageNet	NES	3%	0%	0%	100%	92%	0%
	Boundary	27%	18%	0%	38%	46%	0%
	Square	1%	0%	0%	84%	87%	0%
	HSJA	0%	0%	0%	50%	91%	0%
	QEBA	0%	0%	0%	50%	96%	0%
	SurFree	2%	0%	0%	93%	100%	0%
CelebaHQ	NES	40%	47%	0%	100%	97%	8%
	Boundary	96%	54%	0%	73%	70%	0%
	Square	6%	9%	5%	96%	100%	0%
	HSJA	0%	0%	0%	77%	90%	3%
	QEBA	0%	0%	0%	93%	100%	8%
	SurFree	0%	7%	0%	98%	100%	0%
	Avg	7.79%	7.72%	0.29%	77.63%	87.72%	4.08%

step. OARS is designed to adapt the attack direction and step size based on the decision of the defense model to reduce the detection rate of the defense. However, QPA can effectively detect each attempt and make the attack fail. The ASR of Square and QEBA on CIFAR10 are the highest, which are 20% and 18% respectively. This is because these attack algorithms perform extremely well on some samples and can generate adversarial examples within 10 queries, which is hard for the defense to detect.

6.3. Efficiency

We evaluate the efficiency of QPA by comparing the throughput and latency with our baselines and our system without dynamic management. We deploy the three systems on the same server with 128-core Intel(R) Xeon(R) Platinum 8358 CPU and 488GB memory. We record the total processing time for each instance sequence and the latency of each query during the experiments in Section 6.2. We calculate the average throughput and latency for each system. We show our results in Figure 3 and Figure 4.

As shown in Figure 3, QPA achieves the highest throughput among the three systems. The throughput of QPA is $7.67\times$ higher than BlackLight and $2.25\times$ higher than PIHA. The larger the image, the more significant the throughput improvement. In Figure 4, QPA has the lowest latency among the three systems. The average latency of QPA is 9.87ms for

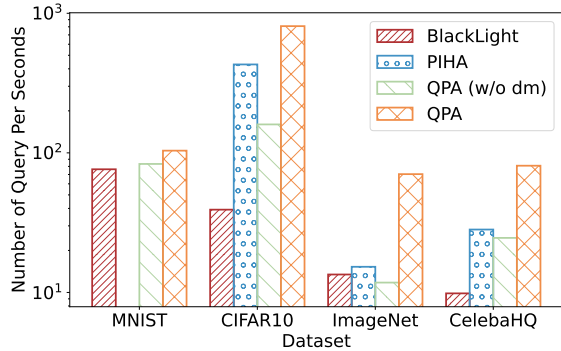


Figure 3: Throughput of QPA compared with BlackLight, PIHA and QPA without dynamic management. The throughput is the number of queries processed per second.

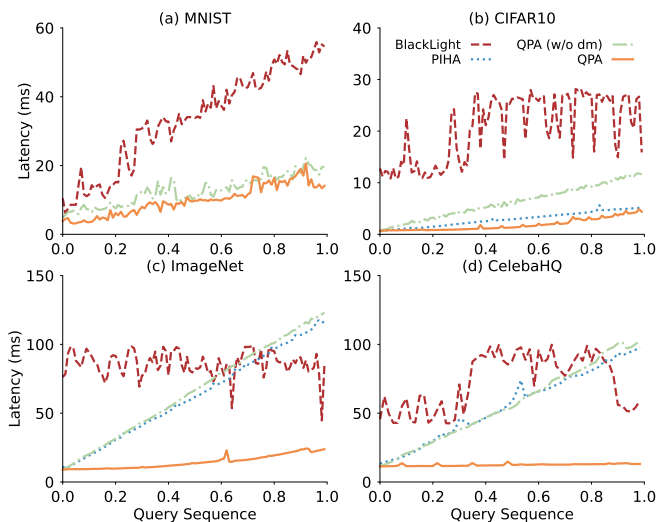


Figure 4: Latency of QPA compared with BlackLight, PIHA and QPA without dynamic management. The latency is the average time taken to process a query. The x-axis represents the proportion of the total sequence and the y-axis represents the response latency. Each point in the graph represents the average latency of 500 queries.

MNIST, 1.86ms for CIFAR10, 14.51ms for ImageNet and 12.45ms for CelebaHQ, which is 3.39 - 11.09 \times faster than BlackLight and 1.59 - 4.49 \times faster than PIHA. The dynamic management of our system improves 3.81 \times the throughput and 1.29 - 4.56 \times the latency compared with the system without dynamic management. The throughput and latency on CIFAR10 are better than that on MNIST because we use the similarity algorithm of BlackLight on MNIST, which is less efficient than the similarity algorithm of PIHA that we use in other datasets. The results on the other three datasets show our system is more efficient than PIHA. The reason our system performs better than the other two baselines is that QPA deploys graph eviction strategy to reduce the features stored in the memory so that it reduces the time to find the closest query in history.

6.4. Insight Verification

While the QPA has demonstrated impressive performance in detecting both non-adaptive and adaptive attacks, it remains crucial to validate the key insight that sequence features are more robust than individual features. To this end, we have conducted the following experiments.

Individual Feature vs. Sequence Feature. We first compare the statics of individual features and sequence features in detecting NES attack with OARS strategy, denoting as NES-OARS, on the ImageNet. We deploy QPA and the other two baselines to defend against the NES-OARS attacks, as configured in the adaptive attacks experiments. We record the individual features for each query during the attack procedure. For QPA, we also collect the normalized anomaly score of the query provenance graph to which the new query is appended as the sequence feature.

Figure 5 demonstrates that the sequence feature of QPA is more robust than individual features in detecting adaptive attacks. The NES-OARS attack successfully evaded BlackLight and PIHA after 3,075 and 2,839 queries but failed to evade QPA after 614 query attempts due to the lack of feasible directions. For individual similarity-based detection, 97.40% of the queries evade BlackLight’s detection and 98.66% PIHA’s. Although all individual features collected during QPA’s detection are below the detection threshold, QPA’s sequence feature still successfully detects the attack. As the attack proceeds, the sequence feature of QPA gradually increases. This indicates that while adaptive attacks can adjust their perturbations to evade the threshold, they struggle to conceal the sequence feature. These results confirm that sequence features can capture the attack pattern more effectively than individual features.

Statistics Distribution. To confirm the distinctiveness of sequence features from individual features, we analyzed the anomaly scores of query provenance graphs, comparing sequences of benign and adversarial queries. In our experiments, we randomly sampled an instance from the ImageNet as the victim for each type of attack using OARS strategy, subsequently recording the anomaly score of the query provenance graph to which the new query is appended during the attack procedure. Given that attack sequences encompass hundreds to thousands of queries, we present the results pertaining to the first five hundred queries in Figure 6. Our analysis reveals that the query provenance features of benign queries are magnitudes smaller than those of the attack queries, with a substantial 84% of benign queries exhibiting no discernible query provenance. This absence of query provenance among benign queries is attributable to their lack of interrelatedness, resulting in a query provenance graph that reflects random, disparate behavior. Conversely, the anomaly score for adversarial queries escalates as successive queries arrive, a trend that is a direct consequence of their consecutive generation. This analysis underscores the statistical distinctiveness of sequence features from individual features, providing a basis for statistical analysis to detect adaptive attacks.

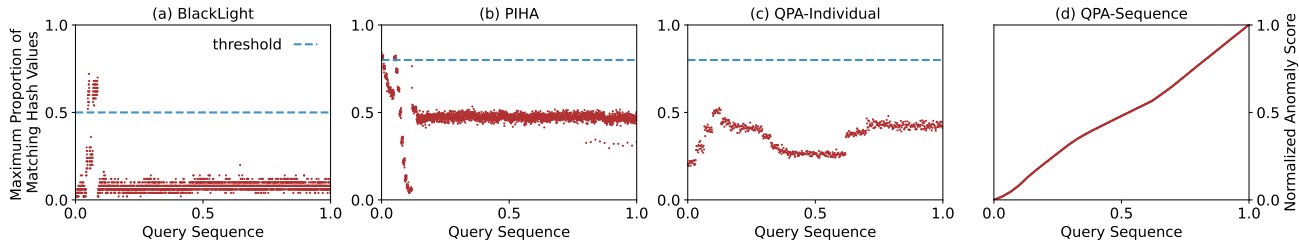


Figure 5: We compare the individual feature in existing SDMs with the sequence feature of our system in detecting NES-OARS. The x-axis represents the number of queries and the y-axis represents the maximum proportion of matched hash values for the individual feature distance and normalized anomaly score for sequence feature distance. (a) and (b) are the results of our two baselines, (c) is the individual features of our system and (d) is the sequence feature of our system. The blue dashed line represents the detection threshold.

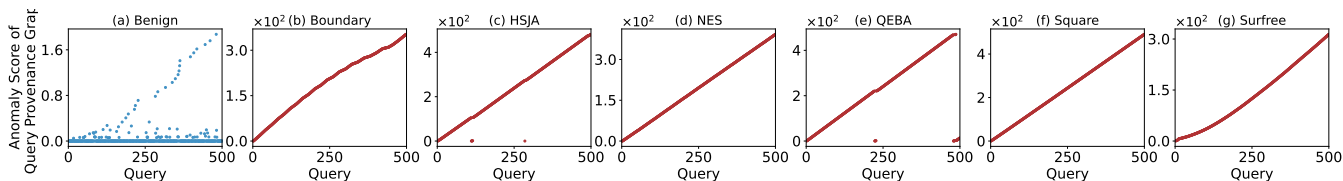


Figure 6: The statistics distribution of the query provenance graphs' anomaly score collected during the attacks with OARS strategy. We show the anomaly score of each query in the first 500 queries of benign and six attack query sequences. The x-axis denotes the number of queries, and the y-axis represents the anomaly score of the query provenance graph for each query.

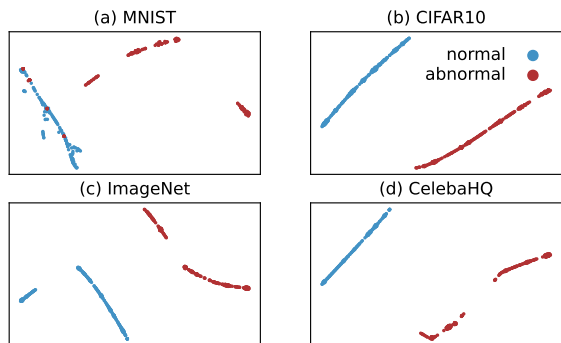


Figure 7: T-SNE visualization of the graph embedding. The blue points represent the normal query provenance graphs and the red points represent the anomaly ones. The visualization results show that the graph embedding can effectively distinguish the anomaly query provenance graphs from the normal query provenance graphs.

Graph Embedding Visualization. To validate the effectiveness of the graph classifier in distinguishing sequence features from individual features, we visualized the graph embeddings of query provenance graphs. We collect the outputs of statistics analysis from 100 instances in the experiments of NES-OARS for each dataset in Section 6.2. Using the pre-trained graph classifier, we extracted the graph embeddings of these query provenance graphs. We then use the t-SNE algorithm for visualization. As shown in Figure 7, the query provenance graph of the normal queries is clearly delineated from the anomalous query provenance graph. This visualization underscores the efficacy of graph em-

beddings in differentiating normal query provenance graphs from anomalous ones, indicating the robustness of sequence features in detecting adaptive attacks.

6.5. Hyperparameters and Ablation Study

Hyperparameters Setting. We evaluate the setting of hyperparameters in QPA to show the impact of each hyperparameter on the detection performance. We choose the default hyperparameters using the optimal experiment results on the four datasets with the HSJA attack. We record the detection precision, recall and F1-Score as metrics to evaluate the detection performance. For each setting, we run the experiments 20 times and record the average results. We show the results in Figure 8.

Top K graphs. We use the parameter K to control the number of graphs stored in the cache. The larger the K setting, the more features will be stored in the memory, which will consume more memory. We evaluate the impact of K on the detection performance. As shown in Figure 8(a), the detection performance increases as the K increases and achieves the best performance when $K = 20$. The reason is that the more graphs stored in the cache, the more features can be used to detect the attack pattern. However, the detection efficiency decreases when K increases. We set $K = 20$ because it achieves the best average F1-Score on the four datasets.

Minimum graph size s to detect. In QPA, we set a minimum graph size s to limit the size of the input to the graph classifier. The larger the s setting, the longer the TTD. Therefore we evaluate the impact of s on the detection performance so that we can balance the detection performance and TTD.

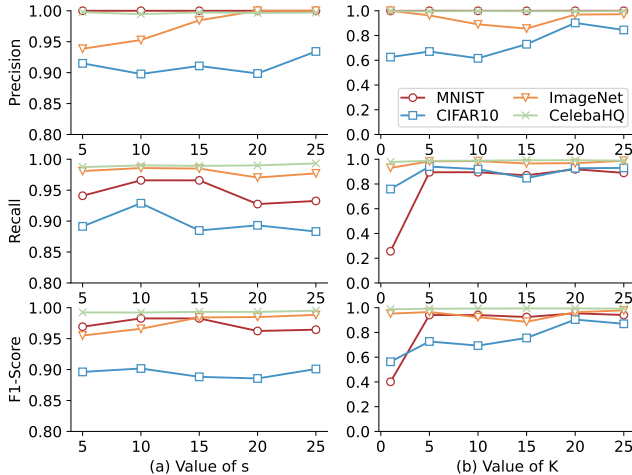


Figure 8: Detection accuracy of our system on different parameter settings.

As shown in Figure 8(b), the detection precision increases with the increase of s . The reason is that as the graph size increases, the graph classifier is more robust to capture the attack pattern. However, the detection recall decreases when s is too large. Because there may be some small graphs that contain the attack pattern but are filtered out by the graph classifier. We set $s = 15$ because it achieves the best average F1-Score on the four datasets.

Ablation Study. Our system incorporates a threshold mechanism to filter normal queries and a graph classifier to enhance detection accuracy. We conducted an ablation study on four datasets under HSJA attacks to evaluate the individual contributions of these components. This study involved removing the threshold mechanism from the graph construction phase and the graph classifier from the QPA phase. We assessed the impact of each modification on detection performance separately, using the performance metrics of the unmodified system as a baseline. Each experimental configuration was tested 100 times to ensure statistical robustness, with the average results being reported for analysis.

Table 5 reveals a substantial decline in detection performance with the removal of the threshold mechanism and the graph classifier. The average precision for detection falls by 70.41% and 61.99% respectively. Correspondingly, the average recall for detection decreases by 42.86% and 12.76%. Additionally, the false positive rate (FPR) increases from 0% to 1.31% and 5.29%. The system encounters complete failure in detection on the ImageNet dataset without the threshold mechanism. This highlights its crucial role in preventing normal queries from connecting to anomalous graphs. Without it, the graph structure and anomaly score distribution are significantly altered, hindering the effectiveness of the QPA. The absence of a graph classifier also compromises the system’s ability to analyze graph structures and identify attack patterns, leading to an increase in false positives. These results emphasize the essential role of both the threshold mechanism and the graph classifier in achieving optimal detection performance.

TABLE 5: Ablation Study on the detection performance of our system. “w/o Threshold” removes the threshold mechanism in the graph construction. “w/o Graph Classifier” removes the graph classifier in the QPA. We regard the detection performance of the original system as the baseline. “Diff” shows the decreases in the detection performance compared with the baseline.

Dataset	w/o Threshold			w/o Graph Classifier		
	Precision	Recall	FPR	Precision	Recall	FPR
MNIST	0.25	0.24	0.75%	0.24	0.86	4.74%
CIFAR10	0.31	0.79	1.79%	0.09	0.60	9.26%
ImageNet	NA	NA	NA	0.39	0.97	3.19%
CelebaHQ	0.31	0.65	1.38%	0.77	0.99	3.98%
Avg	0.29	0.56	1.31%	0.37	0.86	5.29%
Diff	-70.41%	-42.86%	∞	-61.99%	-12.76%	∞

7. Discussion

Evasion: QPA is designed for robust and efficient SDMs. However, due to computational and storage constraints, QPA periodically evicts normal query provenance graphs to disk and resets the query provenance graph storage. This could potentially allow adversaries to evade detection by launching a long-running attack, pausing when they receive a rejection response, and resuming after the system reset.

Despite this, the time required for a successful attack would be impractical for adversaries. For graph eviction, our system is designed to asynchronously evict query provenance graphs to a database, maintaining the query provenance graph in the database without affecting query processing. After eviction, we can asynchronously conduct QPA on the database for global detection, ensuring that graph eviction does not compromise defense. For graph reset, the database is periodically reset to remove stored query provenance graphs, resulting in the loss of historical query features. As shown in Table 1, the average number of queries for an attack is 6721. Assuming adversaries conduct average TTD queries in one reset period, a successful attack would take an average of 333 days if we reset the database every day. Therefore, evading the defense is impractical for adversaries.

Limitations: Our QPA-based SDMs encounters two primary limitations. First, it relies on the similarity of query sequences generated by current query-based black-box attack algorithms. Future research could develop algorithms capable of generating query sequences that do not conform to this assumption. Second, the performance of QPA is influenced by the effectiveness of feature extraction algorithms. While it shows resilience when using existing feature extractors like BlackLight and PIHA, there is room for improvement. For instance, the BlackLight feature extractor exhibits limited effectiveness in detecting Boundary and SurFree attacks. Therefore, the development of more effective feature extractors could enhance the performance and robustness of SDMs.

8. Conclusion

Query-based black-box attacks pose a significant threat to MLaaS systems, with existing techniques achieving nearly 100% ASR. To defend against them, SDMs have been proposed to moderate the input queries based on the similarity between them and the history queries. However, these SDMs are not efficient enough for real-time detection and are vulnerable to sophisticated adaptive attacks, which can bypass the SDMs and achieve high ASR. To this end, we propose QPA for robust and efficient defense against query-based black-box attacks. We model the query sequences as query provenance graphs and design efficient algorithms with dynamic management of query provenance graphs to detect adversarial queries. Our experiments on existing SOTA non-adaptive and adaptive attacks show that QPA can significantly reduce the ASR, maintaining a low false positive rate and minimal overhead.

References

- [1] “Grubbs’s test,” 2022, https://en.wikipedia.org/wiki/Grubbs%27s_test.
- [2] I. Adjabi, A. Ouahabi, A. Benzaoui, and A. Taleb-Ahmed, “Past, present, and future of face recognition: A review,” *Electronics*, vol. 9, no. 8, p. 1188, 2020.
- [3] Amazon., “Amazon rekognition: Automate your image recognition and video analysis with machine learning.” 2024, <https://aws.amazon.com/cn/rekognition/>.
- [4] M. Andriushchenko, F. Croce, N. Flammarion, and M. Hein, “Square attack: a query-efficient black-box adversarial attack via random search,” in *European conference on computer vision*. Springer, 2020, pp. 484–501.
- [5] W. Brendel, J. Rauber, and M. Bethge, “Decision-based adversarial attacks: Reliable attacks against black-box machine learning models,” 2018.
- [6] J. Chen, M. I. Jordan, and M. J. Wainwright, “Hopskipjumpattack: A query-efficient decision-based attack,” in *2020 IEEE Symposium on Security and Privacy (SP)*. IEEE, 2020, pp. 1277–1294.
- [7] S. Chen, N. Carlini, and D. Wagner, “Stateful detection of black-box adversarial attacks,” in *Proceedings of the 1st ACM Workshop on Security and Privacy on Artificial Intelligence*, 2020, p. 30–39.
- [8] S.-H. Choi, J. Shin, and Y.-H. Choi, “Piha: Detection method using perceptual image hashing against query-based adversarial attacks,” *Future Gener. Comput. Syst.*, vol. 145, no. C, p. 563–577, 2023.
- [9] C. A. Choquette-Choo, F. Tramer, N. Carlini, and N. Papernot, “Label-only membership inference attacks,” in *International conference on machine learning*. PMLR, 2021, pp. 1964–1974.
- [10] Clarifai., “The world’s ai: Clarifai computer vision ai and machine learning platform.” 2024, <https://www.clarifai.com/>.
- [11] L. Deng, “The mnist database of handwritten digit images for machine learning research [best of the web],” *IEEE Signal Processing Magazine*, vol. 29, no. 6, pp. 141–142, 2012.
- [12] B. Esmaeili, A. Azmoodeh, A. Dehghantanha, H. Karimpour, B. Zolfaghari, and M. Hammoudeh, “Iiot deep malware threat hunting: From adversarial example detection to adversarial scenario detection,” *IEEE Transactions on Industrial Informatics*, vol. 18, no. 12, pp. 8477–8486, 2022.
- [13] R. Feng, A. Hooda, N. Mangaokar, K. Fawaz, S. Jha, and A. Prakash, “Stateful defenses for machine learning models are not yet secure against black-box attacks,” in *Proceedings of the 2023 ACM SIGSAC Conference on Computer and Communications Security (CCS)*, 2023, p. 786–800.
- [14] D. Ferreira, M. Zacarias, M. Malheiros, and P. Ferreira, “Approaching process mining with sequence clustering: Experiments and findings,” in *Business Process Management: 5th International Conference, BPM 2007, Brisbane, Australia, September 24-28, 2007. Proceedings 5*. Springer, 2007, pp. 360–374.
- [15] A. Geiger, P. Lenz, and R. Urtasun, “Are we ready for autonomous driving? the kitti vision benchmark suite,” in *2012 IEEE Conference on Computer Vision and Pattern Recognition*, 2012, pp. 3354–3361.
- [16] X. Han, X. Yu, T. Pasquier, D. Li, J. Rhee, J. Mickens, M. Seltzer, and H. Chen, “SIGL: Securing software installations through deep graph learning,” in *30th USENIX Security Symposium (USENIX Security 21)*, 2021, pp. 2345–2362.
- [17] N. Iam-On, “Clustering data with the presence of attribute noise: a study of noise completely at random and ensemble of multiple k-means clusterings,” *International journal of machine learning and cybernetics*, vol. 11, no. 3, pp. 491–509, 2020.
- [18] A. Ilyas, L. Engstrom, A. Athalye, and J. Lin, “Black-box adversarial attacks with limited queries and information,” in *International conference on machine learning*. PMLR, 2018, pp. 2137–2146.
- [19] M. M. Islam, H.-C. Yang, T. N. Poly, W.-S. Jian, and Y.-C. J. Li, “Deep learning algorithms for detection of diabetic retinopathy in retinal fundus photographs: A systematic review and meta-analysis,” *Computer Methods and Programs in Biomedicine*, vol. 191, p. 105320, 2020.
- [20] J. Jia, A. Salem, M. Backes, Y. Zhang, and N. Z. Gong, “Memguard: Defending against black-box membership inference attacks via adversarial examples,” in *Proceedings of the 2019 ACM SIGSAC Conference on Computer and Communications Security (CCS)*, 2019, pp. 259–274.
- [21] M. Juuti, S. Szyller, S. Marchal, and N. Asokan, “Prada: protecting against dnn model stealing attacks,” in *2019 IEEE European Symposium on Security and Privacy (EuroS&P)*. IEEE, 2019, pp. 512–527.
- [22] N. Kalchbrenner, L. Espeholt, K. Simonyan, A. v. d. Oord, A. Graves, and K. Kavukcuoglu, “Neural machine translation in linear time,” *arXiv preprint arXiv:1610.10099*, 2016.
- [23] T. Karras, T. Aila, S. Laine, and J. Lehtinen, “Progressive growing of gans for improved quality, stability, and variation,” *arXiv preprint arXiv:1710.10196*, 2017.
- [24] T. S. Kate Follis, Paul Inbar, “Microsoft sequence clustering algorithm.” 2023, <https://learn.microsoft.com/en-us/analysis-services/data-mining/microsoft-sequence-clustering-algorithm?view=asallproducts-allversions>.
- [25] A. Krizhevsky, “Learning multiple layers of features from tiny images,” pp. 32–33, 2009.
- [26] Y. Lecun, L. Bottou, Y. Bengio, and P. Haffner, “Gradient-based learning applied to document recognition,” *Proceedings of the IEEE*, vol. 86, no. 11, pp. 2278–2324, 1998.
- [27] H. Li, X. Xu, X. Zhang, S. Yang, and B. Li, “Qeba: Query-efficient boundary-based blackbox attack,” in *Proceedings of the IEEE/CVF conference on computer vision and pattern recognition*, 2020, pp. 1221–1230.
- [28] H. Li, S. Shan, E. Wenger, J. Zhang, H. Zheng, and B. Y. Zhao, “Blacklight: Scalable defense for neural networks against Query-Based Black-Box attacks,” in *31st USENIX Security Symposium (USENIX Security 22)*, 2022, pp. 2117–2134.
- [29] F. Liu, Y. Wen, D. Zhang, X. Jiang, X. Xing, and D. Meng, “Log2vec: A heterogeneous graph embedding based approach for detecting cyber threats within enterprise,” in *Proceedings of the 2019 ACM SIGSAC Conference on Computer and Communications Security (CCS)*, 2019, pp. 1777–1794.
- [30] L. Liu, S. Lu, R. Zhong, B. Wu, Y. Yao, Q. Zhang, and W. Shi, “Computing systems for autonomous driving: State of the art and challenges,” *IEEE Internet of Things Journal*, vol. 8, no. 8, pp. 6469–6486, 2020.

- [31] T. Maho, T. Furon, and E. Le Merrer, "Surfree: a fast surrogate-free black-box attack," in *Proceedings of the IEEE/CVF Conference on Computer Vision and Pattern Recognition*, 2021, pp. 10430–10439.
- [32] M. Nasr, R. Shokri, and A. Houmansadr, "Machine learning with membership privacy using adversarial regularization," in *Proceedings of the 2018 ACM SIGSAC Conference on Computer and Communications Security (CCS)*, 2018, pp. 634–646.
- [33] —, "Comprehensive privacy analysis of deep learning: Passive and active white-box inference attacks against centralized and federated learning," in *2019 IEEE Symposium on Security and Privacy (SP)*, 2019, pp. 739–753.
- [34] A. Orvieto, S. L. Smith, A. Gu, A. Fernando, C. Gulcehre, R. Pascanu, and S. De, "Resurrecting recurrent neural networks for long sequences," in *International Conference on Machine Learning*. PMLR, 2023, pp. 26670–26698.
- [35] N. Papernot, P. McDaniel, I. Goodfellow, S. Jha, Z. B. Celik, and A. Swami, "Practical black-box attacks against machine learning," in *Proceedings of the 2017 ACM on Asia Conference on Computer and Communications Security (ASIACCS)*, 2017, pp. 506–519.
- [36] A. Rashid and J. Such, "Malprotect: Stateful defense against adversarial query attacks in ml-based malware detection," *IEEE Transactions on Information Forensics and Security*, vol. 18, pp. 4361–4376, 2023.
- [37] P. Recognizer, "Automatic license plate recognition - high accuracy alpr." 2022, <https://platerecognizer.com/>.
- [38] O. Russakovsky, J. Deng, H. Su, J. Krause, S. Satheesh, S. Ma, Z. Huang, A. Karpathy, A. Khosla, M. Bernstein *et al.*, "Imagenet large scale visual recognition challenge," *International journal of computer vision*, vol. 115, pp. 211–252, 2015.
- [39] R. Shokri, M. Stronati, C. Song, and V. Shmatikov, "Membership inference attacks against machine learning models," in *2017 IEEE Symposium on Security and Privacy (SP)*, 2017, pp. 3–18.
- [40] C. Szegedy, W. Zaremba, I. Sutskever, J. Bruna, D. Erhan, I. Goodfellow, and R. Fergus, "Intriguing properties of neural networks," *arXiv preprint arXiv:1312.6199*, 2013.
- [41] Y. Tashiro, Y. Song, and S. Ermon, "Diversity can be transferred: Output diversification for white-and black-box attacks," *Advances in neural information processing systems*, vol. 33, pp. 4536–4548, 2020.
- [42] F. Tramèr, F. Zhang, A. Juels, M. K. Reiter, and T. Ristenpart, "Stealing machine learning models via prediction APIs," in *25th USENIX security symposium (USENIX Security 16)*, 2016, pp. 601–618.
- [43] P. Velickovic, G. Cucurull, A. Casanova, A. Romero, P. Lio, Y. Bengio *et al.*, "Graph attention networks," *stat*, vol. 1050, no. 20, pp. 10–48550, 2017.
- [44] J. Wan, J. Fu, L. Wang, and Z. Yang, "Bounceattack: A query-efficient decision-based adversarial attack by bouncing into the wild," in *2024 IEEE Symposium on Security and Privacy (SP)*. IEEE Computer Society, 2024, pp. 71–71.
- [45] M. Wang and W. Deng, "Deep face recognition: A survey," *Neuro-computing*, vol. 429, pp. 215–244, 2021.
- [46] W. Wang, D. Liang, Q. Chen, Y. Iwamoto, X.-H. Han, Q. Zhang, H. Hu, L. Lin, and Y.-W. Chen, "Medical image classification using deep learning," *Deep learning in healthcare: paradigms and applications*, pp. 33–51, 2020.
- [47] E. W. Weisstein, "Line graph," 2024, <https://mathworld.wolfram.com/LineGraph.html>, From MathWorld—A Wolfram Web Resource.
- [48] S. Yeom, I. Giacomelli, M. Fredrikson, and S. Jha, "Privacy risk in machine learning: Analyzing the connection to overfitting," in *2018 IEEE 31st Computer Security Foundations Symposium (CSF)*, 2018, pp. 268–282.
- [49] H. Yu, K. Yang, T. Zhang, Y.-Y. Tsai, T.-Y. Ho, and Y. Jin, "Cloudleak: Large-scale deep learning models stealing through adversarial examples," in *NDSS*, vol. 38, 2020, p. 102.
- [50] S. Zhang, H. Tong, J. Xu, and R. Maciejewski, "Graph convolutional networks: a comprehensive review," *Computational Social Networks*, vol. 6, no. 1, pp. 1–23, 2019.